***JKPK (JURNAL KIMIA DAN PENDIDIKAN KIMIA)**, Vol. 9, No.1, 2024* *pp. 115-129*
Chemistry Education Study Program, Universitas Sebelas Maret *ISSN 2503-4146*
https://jurnal.uns.ac.id/jkpk *ISSN 2503-4154 (online)*

FUNCTIONALIZATION MESOPOROUS SILICA USING AMINOPROPYLTRIETHOXYSILANE (APTES) AS ADSORBENT FOR REMOVAL Ni (II) FROM AQUEOUS SOLUTION

Ega Hidayani[1], Andriayani[2*], Muhammad Taufik[2]

[1]Postgraduate School, Department of Chemistry, Faculty of Mathematics and Natural Science, University of Sumatera Utara, Medan, Indonesia.
[2]Department of Chemistry, Faculty of Mathematics and Natural Science, University of Sumatera Utara, Medan, Indonesia.

ARTICLE INFO

Keywords:
Adsorption;
APTES,
Mesoporous Silica,
Nickel (II)

Article History:
Received: 2023-03-27
Accepted: 2024-02-26
Published: 2024-03-03

**Corresponding Author*
Email: andriayani@gmail.com
doi:10.20961/jkpk.v9i1.85597

ABSTRACT

This study successfully synthesized mesoporous silica using the template methyl ester ricinoleate (MS-TMR) and further functionalized the MS-TMR surface with 3-aminopropyltriethoxysilane (APTES). The functionalization of MS-TMR with APTES was achieved through a 48-hour grafting method. For the adsorption experiments, 20 mg of both MS-TMR and MS-TMR-APTES adsorbents were employed to remove Ni(II) from aqueous solutions at a concentration of 30 mg/L and pH 6. The objective was to assess the adsorption capacity and to characterize the synthesized adsorbents. Characterization was conducted using Fourier Transform Infrared Spectroscopy (FTIR) and X-ray Diffraction (XRD). FTIR analysis revealed that the MS-TMR adsorbent possessed silanol (Si-OH) and siloxane (Si-O-Si) groups. Conversely, the MS-TMR-APTES adsorbent exhibited additional amine (N-H) and C-H groups after the APTES grafting. XRD results indicated that both samples were amorphous. The concentration of Ni(II) ions was determined using Atomic Absorption Spectroscopy (AAS), which facilitated the calculation of removal percentages and adsorption capacities. MS-TMR achieved a mere 3.54% removal of Ni(II) ions, corresponding to an adsorption capacity of 3.21 mg/g. In contrast, MS-TMR-APTES demonstrated significantly enhanced performance, removing 54.23% of Ni(II) ions with an adsorption capacity of 48.81 mg/g. The findings suggest that APTES-functionalized MS-TMR has considerable potential for removing Ni(II) ions and could be explored further for the adsorption of other heavy metal ions.

How to cite: E. Hidayani, Andriayani, M. Taufik, " Functionalization Mesoporous Silica using Aminopropyltriethoxysilane (APTES) as Adsorbent for Removal Ni (II) from Aqueous Solution," *Jurnal Kimia dan Pendidikan Kimia (JKPK),* vol. 9, no. 1, pp. 115-129, 2024. Available: http://dx.doi.org/10.20961/jkpk.v9i1.85597

INTRODUCTION

The increasing pace of industrial development may contribute significantly to water pollution through industrial wastewater effluent [1]. Industrial waste, containing organic and inorganic pollutants, includes heavy metals, which are particularly hazardous due to their non-biodegradable nature. Commonly found heavy metals in industrial waste include nickel (Ni), zinc (Zn), copper (Cu), chromium (Cr), cadmium (Cd), lead (Pb), mercury (Hg), and arsenic (As). Nickel is notably carcinogenic and can cause a range of health issues, including digestive disorders, lung and kidney problems, and skin dermatitis [2]. A 2022 study highlighted the detrimental respiratory effects of nickel exposure on workers in a nickel refining factory, showing that long-term exposure to

nickel dust and fumes significantly increases the risk of developing respiratory diseases such as bronchitis, asthma, and lung cancer [3]. These health risks underscore the urgent need for effective mitigation strategies to safeguard workers in nickel-related industries and the general public from the adverse effects of nickel pollution.

Nickel is primarily sourced from mining, smelting, machinery processing, chemical production, textiles, and electroplating. The electroplating industry, in particular, utilizes substantial quantities of nickel in its coatings and discharges nickel-rich effluents with concentrations reaching up to 500 mg/L [4], far exceeding the safe limit of 1 mg/L for nickel concentration in water. Exceeding this threshold poses significant environmental and public health risks due to water pollution [5].

The conventional method for Ni(II) removal involves chemical precipitation; however, this treatment is costly and often fails to reduce the residual Ni(II) concentration in the effluent to safe levels [6]. The adsorption technique provides a superior alternative for heavy metal ion removal due to its versatility, high adsorption capacity, operational simplicity, cost-effectiveness, and the potential for adsorbent regeneration [7]. Among various adsorbents, mesoporous silica stands out due to its high surface area, uniform pore size distribution, low production cost, substantial adsorption capacity for pollutants, and the ease with which its surface can be chemically modified to enhance performance [8].

Previous research has documented the synthesis of mesoporous silica using methyl ester ricinoleate with added HCl as an adsorbent, achieving a maximum adsorption capacity of 103.10 mg/g for Cd^{2+} ions and 87.03 mg/g for Cu^{2+} ions [9], [10]. However, the efficiency in removing other heavy metal ions still needs to be improved [11]. Mesoporous silica's lack of diverse functional groups on its surface restricts its application to specific target molecules.

To address this limitation, mesoporous silica's surface can be modified with various ligands such as organic groups, coordination compounds, and nanoparticles to expand its application scope [12]. A common strategy for enhancing adsorbent properties includes surface modification [13]. Specifically, amine group modification is advantageous due to the simplicity of the reaction and its effectiveness in heavy metal removal [14]. Functionalizing mesoporous silica with amine groups allows it to bind several divalent cations, thus exhibiting high adsorption capacity and selectivity for heavy metal ions. The silane coupling agent 3-Aminopropyltriethoxysilane (APTES), characterized by its amine groups, plays a crucial role in this process [15].

The functionalization of mesoporous silica with APTES results in silane termination within the structure, creating a stable covalent bond between the amine group of APTES and the silanol group on the silica mesopore surface [16]. This chemical modification significantly increases the surface area and pore volume, maximizing the contact area between the adsorbent and the heavy metal ions. Consequently, Ni(II) ions in the solution form coordination complexes with the amine groups on the surface of APTES-functionalized mesoporous silica through chelation [18].

Extensive research has been conducted on APTES-functionalized mesoporous silica for various applications, such as the adsorption of Pb(II), Cu(II), and Cd(II) ions [19], textile dye adsorption [20], and CO_2/H_2O adsorption [21]. However, despite these advancements, studies focusing on Ni(II) adsorption are relatively scarce. This study aims to fill this gap by exploring the adsorption capabilities of APTES-functionalized mesoporous silica for Ni(II) ions, emphasizing the functionalization technique and providing crucial data that can aid in the development of effective and sustainable heavy metal ion removal technologies. Mesoporous silica synthesized using ricinoleate methyl ester from castor oil (*Ricinus communis*) as a template will be functionalized with APTES using the post-synthesis grafting method to integrate amine groups onto the silica mesopore surface. The resulting APTES-functionalized mesoporous silica will be applied as an adsorbent for Ni(II) ions in aqueous solutions.

METHODS

1. Materials

The materials employed in this study include castor oil, distilled water, methanol (CH_3OH), potassium hydroxide (KOH), n-hexane (C_6H_{14}), tetraethylorthosilicate (TEOS), 3-aminopropyltrimethoxysilane (APMS), deionized water, hydrochloric acid (HCl), toluene, 3-aminopropyltriethoxysilane (APTES), ethanol (C_2H_5OH), and nickel nitrate hexahydrate ($Ni(NO_3)_2.6H_2O$). These materials were utilized due to their high purity levels, suitable for the chemical processes described.

2. Synthesis of Methyl Ester Ricinoleate from Castor Oil

The methyl ester synthesis from castor oil (Ricinus communis) was performed following established protocols [10]. The process involved transesterification, where 40 grams of castor oil, 86 grams of methanol, and 0.8 grams of KOH as a catalyst were combined in a three-neck flask. This mixture was refluxed at 70°C for four hours. Subsequently, the reaction mixture was extracted with n-hexane, resulting in two phases. The upper phase was washed with distilled water, and the methyl ester was isolated using a rotary evaporator, yielding a pale yellow-colored product. The product's composition was verified by Gas Chromatography-Mass Spectrometry (GC-MS). The prepared methyl ester served as a template for synthesizing mesoporous silica.

3. Synthesis of Mesoporous Silica MS-TMR

The synthesis protocol for mesoporous silica, referred to in the literature, involved the optimization of TEOS and APMS concentrations [22], methanol mass [23], and HCl volume [9]. Initially, 9.04 g of methyl ester ricinoleate was mixed with 150 mL of deionized water, 15 mL of methanol, and 50 mL of 0.1 M HCl and stirred for 30 minutes (mixture A). Concurrently, 12.064 g of TEOS (0.058 mol) and 2.0764 g of APMS (0.0116 mol) were combined and stirred for 15 minutes in a sealed container (mixture B). Mixture B was then added to mixture A, and the combined mixture was stirred for an additional 2 hours. The reaction mixture was aged in an oven at 80°C for 72 hours to allow the formation of porous solids.

Post-aging, the mixture was centrifuged, the solid washed with deionized water, and dried at 60°C. The final product was calcined at 550°C for 6 hours to obtain a white solid, designated as MS-TMR [10].

4. Functionalization of Mesoporous Silica with APTES

The mesoporous silica MS-TMR was functionalized with 3-aminopropyltriethoxysilane (APTES) following a modified post-grafting method referenced from the literature [16]. The process involved placing 1 gram of MS-TMR and 100 mL of dry toluene into a three-neck flask, stirring for 30 minutes. Afterward, 5 mL of APTES was added, and the mixture was refluxed at room temperature under a nitrogen atmosphere for 48 hours. The product was then filtered and washed sequentially with 50 mL of dry toluene and 50 mL of ethanol, followed by drying under vacuum at 80℃ for 20 hours.

5. Characterization

Characterization of the synthesized materials was performed using several techniques. Gas Chromatography-Mass Spectrometry (GC-MS) analysis was carried out on a Trace 1310 GC system with a capillary fused silica column, with the temperature settings ranging from 140°C to 220°C and helium as the carrier gas flowing at 40 to 70 mL/min. Fourier-transform Infrared Spectroscopy (FT-IR) was conducted using a Shimadzu IR Prestige-21 instrument with KBr pellets to identify functional groups on the castor oil methyl esters and silica mesopore surfaces. X-ray Diffraction (XRD) was executed using an E Philip PW 3050/XPert Pro PANalytical system, utilizing Cu Kα radiation (λ = 1.542 Å) with scans at a speed of 2 deg/min over a range of 2θ = 1-15° for low angles and 2θ = 10-90° for wide angles, to assess the crystalline structure of the mesoporous silica.

6. Ni (II) Adsorption

In separate trials, the adsorption study for Ni(II) ions was conducted using 20 mg of MS-TMR and MS-TMR-APTES as adsorbents. Each adsorbent was placed in a 250 mL Erlenmeyer flask containing a $Ni(NO_3)_2.6H_2O$ solution at 30 mg/L concentration. The flask was shaken at 150 rpm for one hour at room temperature. Subsequently, the reaction mixture was filtered, and the filtrate was analyzed using Atomic Absorption Spectroscopy (AAS, iCE 3300). The AAS was equipped with a hollow cathode lamp specific to Ni(II), and the Ni(II) absorption was measured at a wavelength of 232.2 nm. Calibration curves derived from standard solutions of known Ni(II) concentrations were utilized to ensure precise quantification of the residual Ni(II) ions not adsorbed by the silica.

7. Data analysis

The adsorption capacity using mesoporous silica adsorbent was calculated using the following equation:

$$e = \frac{(Co - Ce) \times V}{m} \qquad (1)$$

The percentage removal of Ni (II) metal by mesoporous silica adsorbent was calculated using the following equation:

$$R = \frac{(Co - Ce)}{Co} \times 100\ \% \qquad (2)$$

Where, C_0 (mg/L) is the initial concentration of nickel (II) metal, Ce (mg/L) is the final

concentration of Ni (II) metal. Adsorption capacity (Qe) is the amount of Ni (II) metal adsorbed per mass of mesoporous silica (mg/g). V is the volume of solution (L), and m is the mass of mesoporous silica (g) [24, 25].

RESULTS AND DISCUSSION

1. Synthesis and Characterization of Castor Oil Methyl Ester

Castor oil was chosen as the template for this study due to its wide availability and abundant raw material properties, making it a cost-effective option for biodiesel production. Unlike other vegetable oils, castor oil is unique in that it is the sole source of hydroxylated fatty acids, which are crucial for producing higher yields of methyl esters during the transesterification process [26]. In this reaction, castor oil is transesterified using popular alcohols such as methanol and ethanol, which are the most commonly utilized [27].

The conversion of castor oil into fatty acid methyl esters and other compounds was quantified using Gas Chromatography-Mass Spectrometry (GC-MS). According to the results presented in Table 1, the ricinoleate methyl ester content was determined to be 90.06%, with the remaining 9.94% comprising methyl esters of other fatty acids. This aligns with previous findings indicating that biodiesel derived from castor oil predominantly contains ricinoleic acid, constituting nearly 90% of its composition [28]. The use of high-purity materials is crucial as they are likely to yield methyl esters of superior quality, which in turn could enhance their adsorption capacity, stability, and performance across various applications [29].

The high purity of castor oil methyl ester ensures the uniformity of the template structure necessary for forming mesoporous silica with consistent pore size and morphology [30]. The direct correlation between the purity of castor oil methyl ester and the quality and performance of the synthesized mesoporous silica is pivotal, especially when modified with APTES. Ensuring the silica surface is devoid of contaminants is essential for facilitating a robust bond between the silica matrix and the APTES molecules, optimizing the functionalization process [31].

Table 1. GC–MS analysis for the methyl ester synthesized from castor oil (Ricinus communis)

Retention time (min)	Name	Molecular Formula	Molecular weight	Area (%)
14.231	Hexadecanoic acid, methyl ester	$C_{17}H_{34}O_2$	270	1.03
17.335	9,12-Octadecadienoic acid (Z, Z)-, methyl ester	$C_{19}H_{34}O_2$	294	4.15
17.508	9-Octadecenoic acid (Z)-, methyl ester	$C_{19}H_{36}O_2$	296	3.02
17.607	9-Octadecenoic acid (Z)-, methyl ester	$C_{19}H_{36}O_2$	296	0.47
18.055	Octadecanoic acid, methyl ester	$C_{19}H_{38}O_2$	298	1.28
21.500	Methyl ricinoleate	$C_{19}H_{36}O_3$	312	90.06

The Fourier Transform Infrared Spectroscopy (FT-IR) spectrum of castor oil methyl ester, displayed in Figure 1, reveals several characteristic absorption bands indicative of its molecular structure. An absorption band at 3700 cm^{-1} signifies the presence of hydroxyl (OH) groups. The bands observed at 2922 cm^{-1} and 2855 cm^{-1}

correspond to sp^3 hybridized C-H stretching vibrations, typical of alkyl chains. Notably, the absorption at 1744 cm^{-1} is attributed to the ester functional group (C=O), a key component of the methyl ester structure [32].

Additional bands at 1438 cm^{-1} and 1364 cm-1 indicate alkane groups (C-C) present in mono-, di-, and triglyceride glycerol structures within the methyl esters of castor oil biodiesel. The ether functionalities are represented by bands at 1170 cm^{-1} and 1013 cm^{-1}, associated with C-O and C-O-C stretching vibrations, respectively. The band suggests the presence of a phenyl ring at 857 cm^{-1}, and the characteristic absorption at 723 cm^{-1} is due to methylene groups (CH2) [33].

These hydroxyl groups in the castor oil methyl esters are particularly significant as they provide potential sites for hydrogen bonding with silica precursors during the synthesis of silica mesopores. Such hydrogen bonds facilitate the condensation reactions necessary for forming silica, thereby aiding in creating organic-inorganic hybrid materials [9]. The results from both GC-MS and FT-IR analyses confirm the suitability of castor oil methyl ester as a template for synthesizing mesoporous silica. The role of the methyl ester as a surfactant is crucial; it acts as a template and significantly influences the pore size in the resultant silica structure [34].

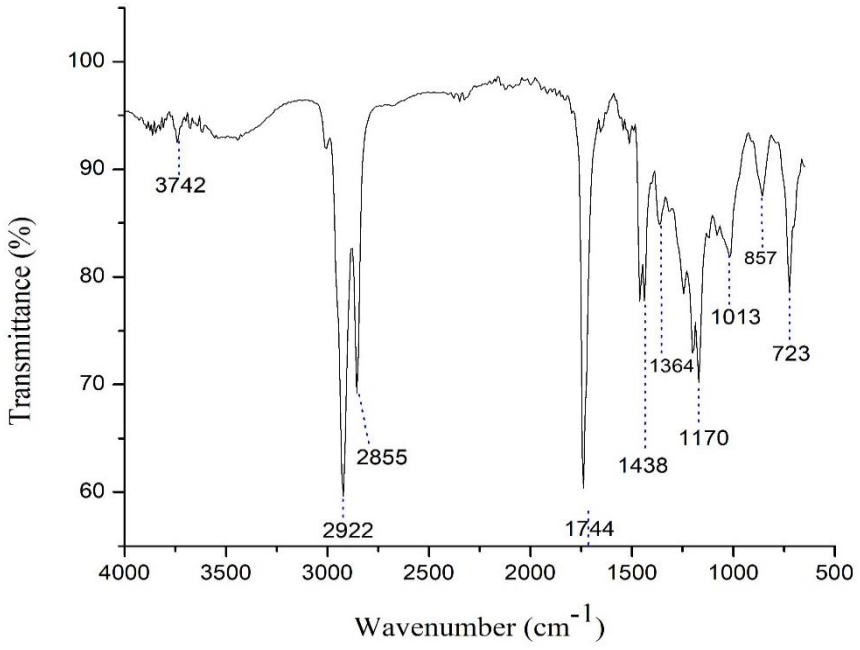

Figure 1. Spectra FT-IR analysis of castor oil methyl ester

2. Characterization of Adsorbent

The functionalization of mesoporous silica with APTES was done through a grafting method involving a 48-hour reflux process in an inert atmosphere. This method heats the reaction mixture to its boiling point and condenses the vapors back into the reaction vessel, ensuring continuous mixing and homogeneous distribution of reactants. Such conditions are critical for effective grafting, as they maintain optimal reaction

parameters over an extended period. Toluene, chosen for its non-polar properties and ability to dissolve various organic compounds, promotes homogeneous mixing with inorganic substrates. The solvent must be dry to avoid the clustering of silanol groups on the mesoporous silica surface, as even minimal amounts of water can trigger this issue [12]. The tri alkoxysilane groups in APTES react with the silica network's silanol groups through alkoxy-silanol interactions.

Successful functionalization is evidenced by the appearance of C-H and N-H groups in the FT-IR analysis, indicating that the amine groups on the silica surface are ready to interact with target molecules. The presence or absence of water during the process influences the distribution and density of functional groups on the silica surface due to the potential hydrolysis of APTES, which can lead to additional reactions and the formation of silanol groups [35].

Figure 2 displays the FT-IR spectra of MS-TMR (black) and MS-TMR-APTES (red). MS-TMR shows an absorption band at 3448 cm^{-1} for hydroxyl groups and a 470 cm^{-1} band for the Si-O-Si bond. Absorption bands at 1110 and 802 cm^{-1} correspond to asymmetric and symmetric vibrations of Si-O-Si, respectively. In the MS-TMR-APTES spectrum, the disappearance of the 979 cm^{-1} band post-grafting indicates that the Si-OH groups have been converted to Si-O groups with amine attachments. The presence of absorption bands at 2924 and 2854 cm^{-1} relates to the vibrations of the C-H group of the APTES propyl chain and the N-H group vibrations at 1565 cm-1, with the C-N bond at 1379 cm-1 confirming successful APTES grafting [36, 37].

Adding amine groups via APTES enhances the adsorption surface area. It improves the selectivity of the adsorbent towards Ni(II) ions, facilitating the formation of stable chelation complexes with metal ions, thus increasing adsorption efficiency [38].

Figure 3 shows the XRD diffractograms of both MS-TMR and MS-TMR-APTES. The analysis shows a broadened peak at 2θ around 22°, and the absence of sharp peaks suggests the maintenance of an amorphous structure, which is crucial for effective adsorption due to the higher surface area and stability provided by amorphous structures [39, 40]. Introducing amine groups from APTES modifies the silica matrix's structural arrangement, as evidenced by new diffraction peaks or changes in peak intensity, demonstrating successful functionalization [41].

Preserving the amorphous structure post-APTES functionalization is key to maximizing the adsorbent's application performance, as amorphous materials typically exhibit superior adsorption kinetics and stability under various conditions. However, the synthesis techniques required to maintain this structure can be more complex and costly than those producing crystalline materials [43].

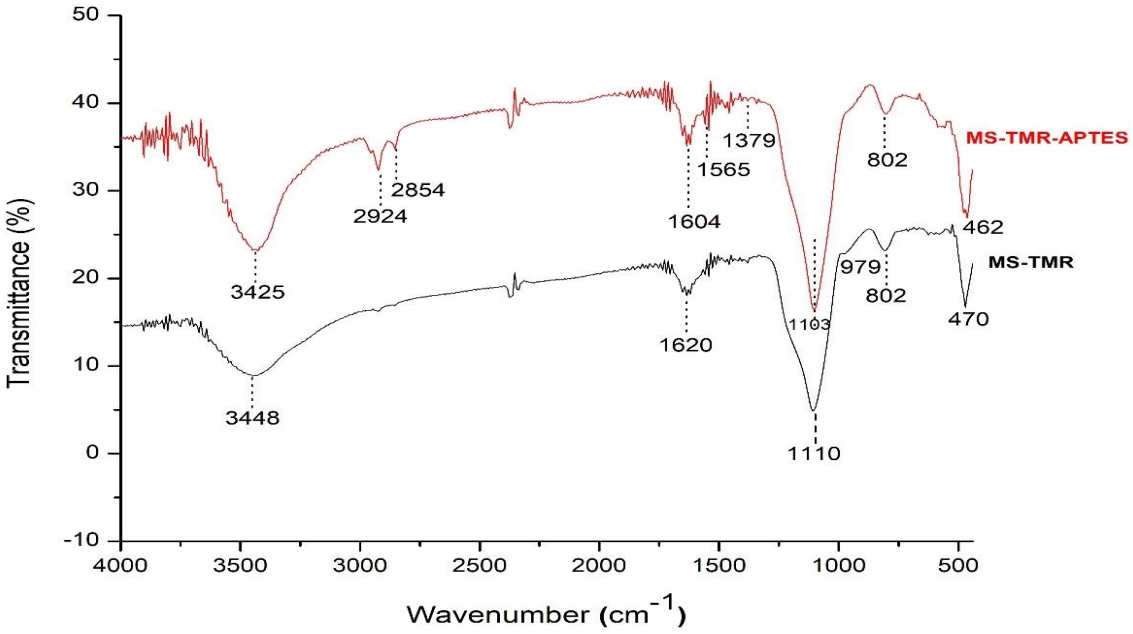

Figure 2. Spectra FT-IR analysis of MS-TMR and MS-TMR-APTES

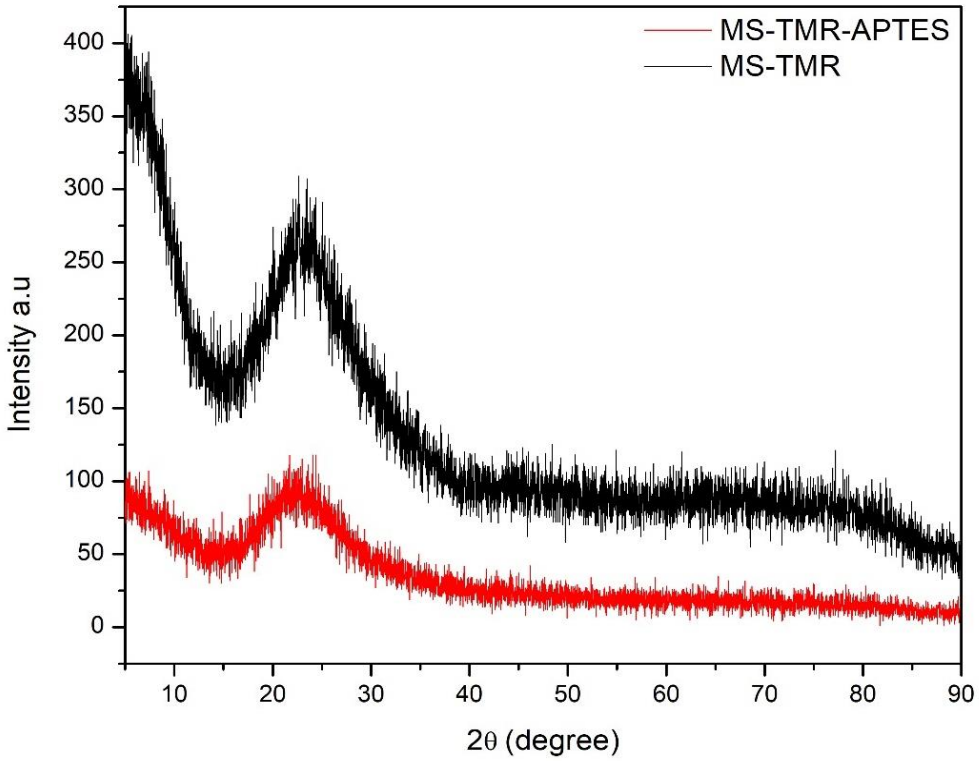

Figure 3. Diffractogram XRD analysis of MS-TMR and MS-TMR-APTES

3. Adsorption Ni (II) Solution

Adsorption experiments were conducted using MS-TMR and MS-TMR-APTES adsorbents, with results detailed in Table 2 and Figure 4. The MS-TMR adsorbent achieved a removal efficiency of 3.54% for Ni (II) metal ions from an aqueous

solution, corresponding to an adsorption capacity of 3.21 mg/g. In contrast, the MS-TMR-APTES adsorbent significantly improved performance, removing 54.23% of Ni (II) metal ions with an adsorption capacity of 48.81 mg/g. The enhanced adsorption efficiency of MS-TMR-APTES is attributed to the amine groups (-NH2) introduced through APTES grafting on the silica surface, which facilitates more effective adsorption than MS-TMR. This improvement aligns with the principles of the Hard Soft Acid Base (HSAB) theory, which suggests that mesoporous silica modified with amine groups, being hard bases, effectively binds the borderline acid nature of Ni (II) metal ions [44].

The amine groups engage in complex formation with target molecules through Lewis acid-base interactions, thereby improving adsorption efficiency. The positively charged amine groups also enhance electrostatic interactions, attracting negatively charged ions. While MS-TMR primarily relies on physical adsorption mechanisms such as Van der Waals forces, MS-TMR-APTES adsorbents facilitate additional chemical interactions, including complexation and electrostatic interactions, due to the presence of amine groups [45].

However, the solution's maximum adsorption capacity is influenced by surface area, pore size, and adsorbate concentration. Although MS-TMR-APTES exhibited increased adsorption capacity for nickel, a saturation point exists beyond which further functionalization or surface modification does not significantly enhance the adsorption capacity. Practical limitations, such as the availability and cost-effectiveness of APTES reagents and the scalability of the synthesis process for large-scale applications, also need consideration [46, 47].

Table 2. Adsorption of Ni (II) by adsorbent

Adsorbent	Co (mg/L)	Ce (mg/L)	Q (mg/g)	R (%)
MS-TMR	30	28,93	3,21	3,54
MS-TMR-APTES	30	13,73	48,81	54,23

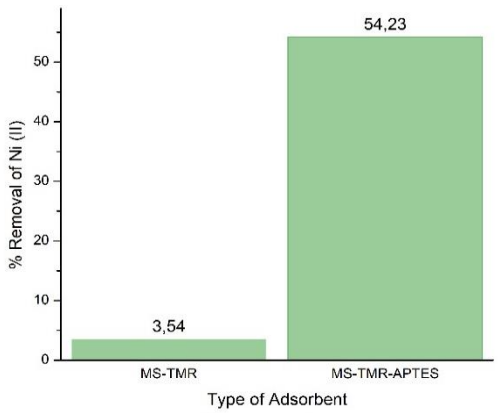

Figure 4. %Removal Ni (II) by Adsorbent

The strong binding affinity of the amine groups to Ni (II) ions results from the formation of stable coordination complexes. However, the affinity of amine groups to other heavy metals may vary based on factors such as charge, size, and metal coordination preferences, affecting the selectivity of MS-TMR-APTES for different heavy metal ions from industrial waste. Metals with higher charges or larger ionic radii are likely to form stronger complexes with amine groups than those with lower charges or smaller ones [45].

Additional comparative data on Ni (II) adsorption using various adsorbents are provided in Table 3, illustrating a broader context for the effectiveness of different adsorption technologies.

Table 3. Comparison of adsorption capacities Ni (II) with other adsorbent

Adsorbent	Q (mg/g)	Ref.
Composite material	199,19	[48]
Nano-SZO	32,10	[49]
MCA	167,55	[50]
MS-TMR	3,21	This Study
MS-TMR-APTES	48,81	This Study

CONCLUSION

The synthesis of mesoporous silica using a methyl ester ricinoleate template (MS-TMR) and its subsequent functionalization with 3-aminopropyltriethoxysilane (APTES), referred to as MS-TMR-APTES, was successfully conducted. Both samples were characterized using Fourier Transform Infrared Spectroscopy (FTIR) and X-ray Diffraction (XRD). FTIR analysis of MS-TMR revealed the presence of Si-OH and Si-O-Si groups, indicative of the silica structure. Following the functionalization with APTES, the appearance of C-H, N-H, and C-N groups in the FTIR spectra confirmed the successful grafting of APTES onto the MS-TMR surface. XRD analysis further corroborated that both products maintained an amorphous structure. MS-TMR and MS-TMR-APTES were evaluated as adsorbents for removing Ni(II) metal ions from an aqueous solution. The experimental conditions were set at a Ni(II) concentration of 30 mg/L, a pH of 6, a contact time of 1 hour, and a stirring speed of 150 rpm. The adsorption performance was quantified using Atomic Absorption Spectroscopy (AAS) to determine the concentration of Ni(II) ions post-adsorption. The results indicated that MS-TMR achieved a removal percentage of 3.54% and an adsorption capacity of 3.21 mg/g. In contrast, the MS-TMR-APTES adsorbent significantly enhanced the removal efficiency to 54.23% and the adsorption capacity to 48.81 mg/g. These findings suggest that the functionalization of mesoporous silica with APTES improves the adsorption efficiency for Ni(II) metal ions and indicates the potential of MS-TMR-APTES to effectively adsorb other heavy metal ions. This enhancement is attributed to the increased interaction capabilities afforded by the amine groups introduced through the APTES functionalization, which facilitate stronger binding with metal ions.

ACKNOWLEDGMENT

This research is financially supported by the Directorate of Research, Technology, and Community Service of the Ministry of Education, Culture, Research, and Technology (DRTPM KEMDIKBUDRISTEK) with Contract Number 79/UN5.2.3.1/PPM/KP-DRTPM/B/2023 .

REFERENCES

[1] W. Jia, H. Xu, Q. Yang, S. Ren, and J. Wang, “Synthesis of anionic gemini surfactant-templated mesoporous silica nanoparticles and its adsorption application for Pb^{2+},” *J. Dispers. Sci. Technol.*, vol. 40, no. 11, pp. 1664–1674, 2019, doi:10.1080/01932691.2018.1535979

[2] I. H. Ifijen *et al.*, “The removal of nickel and lead ions from aqueous solutions using green synthesized silica microparticles,” *Heliyon*, vol. 6, no. 9, 2020, doi: 10.1016/j.heliyon.2020.e04907.

[3] S. Syurin and D. Vinnikov, “Occupational disease predictors in

the nickel pyrometallurgical production: a prospective cohort observation," *J. Occup. Med. Toxicol.*, vol. 17, no. 1, pp. 1–10, 2022, doi: 10.1186/s12995-022-00362-2.

[4] Z. A. Kadhim and A. H. Abbar, "A Novel Bio-electrochemical Cell with Rotating Cylinder Cathode for Cadmium Removal from Simulated Wastewater," *Egypt. J. Chem.*, vol. 65, no. 13, pp. 769–778, 2022, doi:10.21608/EJCHEM.2022.149145.6439

[5] A. Adiningtyas and P. Mulyono, "Kinetika Adsorpsi Nikel (II) dalam Larutan Aqueous dengan Karbon Aktif Arang Tempurung Kelapa," *J. Rekayasa Proses*, vol. 10, no. 2, p. 36, 2016, doi: 10.22146/jrekpros.33335.

[6] T. Li *et al.*, "Industrial-scale highly efficient nickel recovery from electroplating wastewater using resin adsorption followed by aeration mixing acid regeneration," *J. Water Process Eng.*, vol. 58, 2024, doi: 10.1016/j.jwpe.2024.104801.

[7] H. Wu, Y. Xiao, Y. Guo, S. Miao, Q. Chen, and Z. Chen, "Functionalization of SBA-15 mesoporous materials with 2-acetylthiophene for adsorption of Cr(III) ions," *Microporous Mesoporous Mater.*, vol. 292, p. 109754, 2020, doi:10.1016/j.micromeso.2019.109754

[8] J. I. Lachowicz *et al.*, "Adsorption of Cu2+ and Zn2+ on SBA-15 mesoporous silica functionalized with triethylenetetramine chelating agent," *J. Environ. Chem. Eng.*, vol. 7, no. 4, p. 103205, 2019, doi: 10.1016/j.jece.2019.103205.

[9] Andriayani, Marpongahtun, Y. Muis, J. Pakpahan, and A. Daulay, "Stability of mesoporous silica using ricinoleic methyl ester as a template with the addition of HCl and application of Cd2+ adsorption optimized by Box-Behnken design," *RSC Adv.*, vol. 13, no. 11, pp. 7329–7338, 2023, doi: 10.1039/d2ra06973c.

[10] Andriayani, Marpongahtun, Suharman, and A. Daulay, "Synthesis of mesoporous silica with ricinoleic methyl ester (Ricinus communis) as a template for adsorption copper (II) with optimizing Box-Behnken design," *Case Stud. Chem. Environ. Eng.*, vol. 7, p. 100287, 2023, doi: 10.1016/j.cscee.2022.100287.

[11] A. M. Putz *et al.*, "Comparison of structure and adsorption properties of mesoporous silica functionalized with aminopropyl groups by the co-condensation and the post grafting methods," *Materials (Basel).*, vol. 14, no. 3, pp. 1–19, 2021, doi: 10.3390/ma14030628.

[12] J. A. S. Costa, R. A. De Jesus, D. O. Santos, J. B. Neris, R. T. Figueiredo, and C. M. Paranhos, "Synthesis, functionalization, and environmental application of silica-based mesoporous materials of the M41S and SBA-n families: A review," *J. Environ. Chem. Eng.*, vol. 9, no. 3, 2021, doi: 10.1016/j.jece.2021.105259.

[13] G. Zhang, T. Wang, Z. Xu, M. Liu, C. Shen, and Q. Meng, "Synthesis of

amino-functionalized Ti3C2TxMXene by alkalization-grafting modification for efficient lead adsorption," *Chem. Commun.*, vol. 56, no. 76, pp. 11283–11286, 2020, doi: 10.1039/d0cc04265j.

[14] S. J. Mousavi, M. Parvini, and M. Ghorbani, "Adsorption of heavy metals (Cu2+ and Zn2+) on novel bifunctional ordered mesoporous silica: Optimization by response surface methodology," *J. Taiwan Inst. Chem. Eng.*, vol. 84, pp. 123–141, 2018, doi: 10.1016/j.jtice.2018.01.010.

[15] J. Isasi, P. Arévalo, E. Martin, and F. Martín-Hernández, "Preparation and study of silica and APTES–silica-modified NiFe2O4 nanocomposites for removal of Cu2+ and Zn2+ ions from aqueous solutions," *J. Sol-Gel Sci. Technol.*, vol. 91, no. 3, pp. 596–610, 2019, doi: 10.1007/s10971-019-05067-3.

[16] J. de O. N. Ribeiro *et al.*, "Role of the type of grafting solvent and its removal process on APTES functionalization onto SBA-15 silica for CO2 adsorption," *J. Porous Mater.*, vol. 26, no. 6, pp. 1581–1591, 2019, doi: 10.1007/s10934-019-00754-6.

[17] D. Flores, C. R. G. C. Marisa R. Almeida, and S. S. B. and C. M. Granadeiro, "Tailoring of Mesoporous Silica-Based Materials for Enhanced Water Pollutants Removal," *Molecules*, vol. 28, p. 4038, 2023, doi: 10.3390/molecules28104038.

[18] N. G. Kobylinska, V. G. Kessler, G. A. Seisenbaeva, and O. A. Dudarko, "In situ Functionalized Mesoporous Silicas for Sustainable Remediation Strategies in Removal of Inorganic Pollutants from Contaminated Environmental Water," *ACS Omega*, vol. 7, no. 27, pp. 23576–23590, 2022, doi: 10.1021/acsomega.2c02151.

[19] A. Shahbazi, H. Younesi, and A. Badiei, "Functionalized SBA-15 mesoporous silica by melamine-based dendrimer amines for adsorptive characteristics of Pb(II), Cu(II) and Cd(II) heavy metal ions in batch and fixed bed column," *Chem. Eng. J.*, vol. 168, no. 2, pp. 505–518, 2011, doi: 10.1016/j.cej.2010.11.053.

[20] V. Rizzi, J. Gubitosa, P. Fini, S. Nuzzo, and P. Cosma, "Amino-grafted mesoporous MCM-41 and SBA-15 recyclable adsorbents: Desert-rose-petals-like SBA-15 type as the most efficient to remove azo textile dyes and their mixture from water," *Sustain. Mater. Technol.*, vol. 26, p. e00231, 2020, doi: 10.1016/j.susmat.2020.e00231.

[21] G. L. Avellaneda, R. Denoyel, and I. Beurroies, "CO2/H2O adsorption and co-adsorption on functionalized and modified mesoporous silicas," *Microporous Mesoporous Mater.*, vol. 363, 2024, doi:10.1016/j.micromeso.2023.112801

[22] Andriayani, H. Nainggolan, M. Taufik, S. Simamora, and N. Sofyan, "The effect concentration of tetraethylorthosilicate and variation HCl 0.1M for synthesis mesoporous silica using oleic acid as template and 3-aminopropyltrimethoxysilane as co-structure directing Agent," *J.*

Phys. Conf. Ser., vol. 1116, no. 4, pp. 0–8, 2018, doi:10.1088/17426596/1116/4/042006.

[23] A. D. Andriayani, Marpongahtun, Yugia Muis, Jessica Mardela Pakpahan, "Methanol Mass Variation of Mesoporous Silica Synthesis Using Ricinoleic Methyl Ester as a Template," vol. 57, no. 1, 2022, doi:10.35741/issn.0258-2724.57.1.55.

[24] Y. D. Ngapa and J. Gago, "Optimizing of Competitive Adsorption Methylene Blue and Methyl Orange using Natural Zeolite from Ende-Flores," *JKPK (Jurnal Kim. dan Pendidik. Kim.*, vol. 6, no. 1, p. 39, 2021, doi: 10.20961/jkpk.v6i1.46132.

[25] E. P. Kuncoro, C. Deborah, P. Matondang, M. Fajar, and H. Darmokoesoemo, "Use Of Placuna Placenta Shells As Green Adsorbent For Pb (II) Ions Sequestration From Aqueous Solution," vol. 8, no. 3, pp. 310–323, 2023, doi: 10.20961/jkpk.v8i3.80152.

[26] N. Sánchez, J. M. Encinar, S. Nogales, and J. F. González, "Biodiesel production from castor oil by two-step catalytic transesterification: Optimization of the process and economic assessment," *Catalysts*, vol. 9, no. 10, 2019, doi: 10.3390/catal9100864.

[27] M. G. Sohini Mukherjee, "Studies on Performance Evaluation of a Green Plasticizer Made by Enzymatic Esterification of Furfuryl Alcohol and Castor Oil Fatty Acid," *Carbohydr. Polym.*, 2016, doi: 10.1016/j.carbpol.2016.10.075.

[28] C. L. Palconite *et al.*, "Optimization and characterization of bio-oil produced from Ricinus communis seeds via ultrasonic-assisted solvent extraction through response surface methodology," *Sustain. Environ. Res.*, vol. 28, no. 6, pp. 444–453, 2018, doi: 10.1016/j.serj.2018.07.006.

[29] N. D. Wela and A. D. Wela, "Study of Reaction Conditions for the Synthesis of Methyl Oleic from Used Cooking Oil," *Akta Kim. Indones.*, vol. 6, no. 1, p. 41, 2021, doi: 10.12962/j25493736.v6i1.8106.

[30] A. Andriayani, M. Marpongahtun, S. Suharman, and A. Daulay, "Application mesoporous silica with methyl ester ricinoleate castor oil (Ricinus communis) as template in absorbent of Cd ions," in *AIP Conference Proceedings*, 2023, vol. 2626, no. 1.

[31] B. M. Estevão, I. Miletto, N. Hioka, L. Marchese, and E. Gianotti, "Mesoporous Silica Nanoparticles Functionalized with Amino Groups for Biomedical Applications," *ChemistryOpen*, vol. 10, no. 12, pp. 1251–1259, 2021, doi: 10.1002/open.202100227.

[32] R. K. Elango, K. Sathiasivan, C. Muthukumaran, V. Thangavelu, M. Rajesh, and K. Tamilarasan, "Transesterification of castor oil for biodiesel production: Process optimization and characterization," *Microchem. J.*, vol. 145, pp. 1162–1168, 2019, doi: 10.1016/j.microc.2018.12.039.

[33] A. M. A. Attia, M. Nour, A. I. El-Seesy, and S. A. Nada, "The effect of castor oil methyl ester blending ratio on the environmental and the combustion characteristics of diesel engine under standard testing conditions," *Sustain. Energy Technol. Assessments*, vol. 42, 2020, doi: 10.1016/j.seta.2020.100843.

[34] S. Ghotekar, S. Pansambal, K. Pagar, O. Pardeshi, and R. Oza, "Synthesis of CeVO 4 nanoparticles using sol-gel auto combustion method and their antifungal activity," vol. 3, no. 2, pp. 189–196, 2018, doi: 10.22036/ncr.2018.02.008.

[35] J. J. Gutiérrez Moreno, K. Pan, Y. Wang, and W. Li, "Computational Study of APTES Surface Functionalization of Diatom-like Amorphous SiO2 Surfaces for Heavy Metal Adsorption," *Langmuir*, vol. 36, no. 20, pp. 5680–5689, 2020, doi: 10.1021/acs.langmuir.9b03755.

[36] I. Puspita Sari and M. Bachri Amran, "Sintesis dan Karakterisasi SiO2@APTES-IIP Sebagai Material Fungsional Penjerap Ion Kadmium(II)," *IJCA (Indonesian J. Chem. Anal.*, vol. 4, no. 1, pp. 18–29, 2021, doi: 10.20885/ijca.vol4.iss1.art3.

[37] J. M. Kolle and A. Sayari, "Dry gel grafting of mesoporous silica: Application to amine-based CO2 adsorbents," *Microporous Mesoporous Mater.*, vol. 343, no. August, p. 112195, 2022, doi:10.1016/j.micromeso.2022.112195

[38] R. Singhon, C. Ii, N. Ii, F. Colloidal, and S. Particles, "Adsorption of Cu (II) and Ni (II) Ions on Functionalized Colloidal Silica Particles Model Studies for Wastewater To cite this version : Adsorption of Cu (II) and Ni (II) Ions on Functionalized Colloidal Silica Particles Model Studies for Wastewate," 2017.

[39] S. Xie *et al.*, "Synthesis of polyaniline-titania nanotube arrays hybrid composite via self-assembling and graft polymerization for supercapacitor application," *Electrochim. Acta*, vol. 120, pp. 408–415, 2014, doi:10.1016/j.electacta.2013.12.067

[40] R. Kishor and A. K. Ghoshal, "APTES grafted ordered mesoporous silica KIT-6 for CO2 adsorption," *Chem. Eng. J.*, vol. 262, pp. 882–890, 2015, doi: 10.1016/j.cej.2014.10.039.

[41] S. Wongsakulphasatch, W. Kiatkittipong, J. Saiswat, B. Oonkhanond, A. Striolo, and S. Assabumrungrat, "The adsorption aspect of Cu2 + and Zn2 + on MCM-41 and SDS-modified MCM-41," *Inorg. Chem. Commun.*, vol. 46, pp. 301–304, 2014, doi: 10.1016/j.inoche.2014.06.029.

[42] B. Dziejarski, J. Serafin, K. Andersson, and R. Krzyżyńska, "CO2 capture materials: a review of current trends and future challenges," *Mater. Today Sustain.*, vol. 24, 2023, doi: 10.1016/j.mtsust.2023.100483.

[43] M. Sypabekova, A. Hagemann, D. Rho, and S. Kim, "Review: 3-Aminopropyltriethoxysilane

(APTES) Deposition Methods on Oxide Surfaces in Solution and Vapor Phases for Biosensing Applications," *Biosensors*, vol. 13, no. 1, 2023, doi: 10.3390/bios13010036.

[44] M. D. Pratiwi, P. Taba, and Y. Hala, "Pemanfaatan Silika Mesopori MCM-48 Termodifikasi 3-Aminopropiltrimetoksisilan Sebagai Adsorben Logam Berat Ni (II)," no. 2, pp. 1–8, 2015.

[45] V. R. Dugyala, J. S. Muthukuru, E. Mani, and M. G. Basavaraj, "Role of electrostatic interactions in the adsorption kinetics of nanoparticles at fluid-fluid interfaces," *Phys. Chem. Chem. Phys.*, vol. 18, no. 7, pp. 5499–5508, 2016, doi: 10.1039/c5cp05959c.

[46] P. N. E. Diagboya and E. D. Dikio, "Silica-based mesoporous materials; emerging designer adsorbents for aqueous pollutants removal and water treatment," *Microporous Mesoporous Mater.*, vol. 266, no. March, pp. 252–267, 2018, doi:10.1016/j.micromeso.2018.03.008

[47] R. Narayan, U. Y. Nayak, A. M. Raichur, and S. Garg, "Mesoporous silica nanoparticles: A comprehensive review on synthesis and recent advances," *Pharmaceutics*, vol. 10, no. 3, pp. 1–49, 2018, doi:10.3390/pharmaceutics10030118.

[48] M. R. Awual *et al.*, "Ligand based sustainable composite material for sensitive nickel(II) capturing in aqueous media," *J. Environ. Chem. Eng.*, vol. 8, no. 1, 2020, doi: 10.1016/j.jece.2019.103591.

[49] R. Garg *et al.*, "Biosynthesized silica-based zinc oxide nanocomposites for the sequestration of heavy metal ions from aqueous solutions," *J. King Saud Univ. - Sci.*, vol. 34, no. 4, p. 101996, 2022, doi: 10.1016/j.jksus.2022.101996.

[50] M. E. Awual *et al.*, "Ligand imprinted composite adsorbent for effective Ni (II) ion monitoring and removal from contaminated water," *J. Ind. Eng. Chem.*, vol. 131, no. November 2023, pp. 585–592, 2024, doi: 10.1016/j.jiec.2023.10.062.